Materials Research. 2025; 28: e20250368
DOI: https://doi.org/10.1590/1980-5373-MR-2025-0368

Laser Butt Welding of Thin AZ31B Magnesium Alloy Sheets with and without Beam Oscillation

Hao Chen*[a,b], *QunYue Gao*[a,b], *Sheng Ye*[c], *Wen Zhu*[a,b], *Yanfei Chen*[a,b], *Zhengqiang Zhu*[a,b]

[a] *Nanchang University, School of Advanced Manufacturing, 330031, Nanchang China.*
[b] *Nanchang University, Jiangxi Key Laboratory of Intelligent Robot, 330031, Nanchang, China.*
[c] *Jiangxi Biotech Vocational College, 330200, Jiangxi, Nanchang, China.*

Received: March 16, 2025; Revised: July 02, 2025; Accepted: July 18, 2025

Magnesium (Mg) alloys are widely used in electronics, automotive, and aerospace industries due to their lightweight, high specific strength, and excellent damping properties. Laser welding, with its high energy density and precise heat control, shows great potential in addressing the challenges of welding thin Mg alloy sheets. This study investigates the laser butt welding of 1 mm thick AZ31B Mg alloy sheets, comparing the effects of welding with and without beam oscillation using tools such as super-depth optical microscope (OM) and scanning electron microscope (SEM). Experimental results indicate that beam oscillation significantly improves weld uniformity, refines the microstructure, and reduces welding defects such as porosity. Stress-strain analysis shows that both methods achieve high strength in 1 mm AZ31B laser welding, with fractures occurring at the weld joint. The non-oscillated weld exhibits strength of approximately 76% of the base metal, while the oscillated weld achieves 85%. However, tensile elongation for both welding methods shows significant decrease compared to the base matel. Fracture surface analysis reveals dimples on the fracture surfaces of both the base metal and the welds. However, both welds exhibit porosity, with fewer pores observed in oscillated welds, demonstrating its superiority over non-oscillated welding. These findings confirm that laser beam oscillation is an effective technique for achieving high-quality welding of thin Mg alloy sheets.

Keywords: *Magnesium alloy, Laser welding, Butt welding, Welding quality.*

1. Introduction

Being the lightest structural metal, Mg alloy possesses the merit of high specific strength, specific stiffness as well as shock absorption, which is advantageous in attaining weight reduction and energy conservation for the fields of electronics, automobiles and aerospace[1,2]. However, the poor weld ability of Mg alloy making the welded joints present various,defects like coarsen-grain, pores, and element evaporation loss. The solidification crack is easily caused by the low-melting-point eutectic in the Mg weld due to its high thermal conductivity, low hydrogen solid solubility, and easy oxidation[3,4]. Therefore, how to achieve high quality welding of Mg alloy becomes one of the most concerning issues.

Owing to the high energy density and low heat input, laser welding has exhibited its great advantages of faster speeds, smaller heat - affected zones (HAZ), and increased penetration depth, and thus has potential for the welding of Mg alloy[5]. Xu et al.[6] conduct different parameters laser beam welding on 4.0 mm thick AZ31B Mg alloy sheets; they found that the formation of fine grains in weld zone and uniformly distributed fine precipitates were the main reasons for superior tensile properties of these joints. Zhang et al.[7] utilize the sinusoidal power modulation in welding 3mm thick AZ31B magnesium alloy by laser welding, they found that, compared with the results from the laser welding with a constant power, modulating the power in a sinusoidal waveform not only increased the width and length of the molten pool, but also increased the volume of melting materials. In the laser welding research of Hao et al.[8] on the circular beam oscillation of 2.0 mm thick AZ31B magnesium alloy, they found that under given parameters, low frequency oscillation and small radius oscillation are beneficial to the appearance of the weld. Zhang et al.[9] employed a power-modulated oscillating laser (PMOL) to weld 3 mm thick AZ31B magnesium alloy workpieces. Their findings revealed that, compared to conventional laser welding or circular oscillation laser welding, PMOL not only significantly increased weld penetration and improved laser energy coupling efficiency but also enhanced the mechanical properties of the weld.

Beyond optimizing welding quality through parameter adjustments in laser welding, alternative approaches can also be utilized to achieve superior results. For instance, Jiang et al.[10] investigated the welding of 10 mm thick magnesium alloy plates in a vacuum environment. Their study demonstrated that under a vacuum pressure of 10 kPa, the weld penetration depth increased, the weld width narrowed and became

*e-mail: zhuzhq01@126.com
Associate Editor: Aloisio Klein.
Editor-in-Chief: Luiz Antonio Pessan.

more uniform, and the weld exhibited reduced porosity along with a smaller average grain size. In the research on ultrasonic assisted laser welding of AZ31B magnesium alloy by Lei et al.[11], it was found that this welding technique can improve the welding characteristics of AZ31B magnesium alloy, and the microstructure of the weld zone is mainly composed of α-Mg matrix and brittle phase β-$Mg_{17}Al_{12}$.

Furthermore, in the hybrid welding process like the laser-arc hybrid welding of AZ31B magnesium alloy, the advantages of both laser welding and arc welding are skillfully integrated, and thus a series of remarkable and prominent characteristics are presented[12]. In the research on laser - arc hybrid welding of 5.4 mm thick AZ31B magnesium alloy by Gao et al.[13], it was found that this welding technique has the ability to restrain the undercut and pore defects in magnesium alloy welding. Hao et al.[14] conducted oscillating laser - arc hybrid welding on 5.4mm - thick AZ31B magnesium alloy sheets with different parameters, they found that in the oscillating laser - arc hybrid welding, the axial pressure of the laser beam and the arc, as well as the shear stress of the oscillating laser beam, jointly act to promote the formation of twins. Meng et al.[15] carried out laser-arc hybrid welding on 4mm AZ31B magnesium alloy sheets with a new inscribed double-circle oscillation pattern,and they found it improved laser energy distribution uniformity, improved weld tensile strength and elongation. Although laser - arc hybrid welding shows advantages in the welding of AZ31B magnesium alloy, laser welding still has research significance in the splicing welding of magnesium alloy thin plates. For magnesium alloy thin plates with strict requirements for heat - affected zones, the precise energy control of laser welding can minimize heat damage. Moreover, in the micro - welding scenarios of magnesium alloy thin plates, laser welding can achieve higher precision and better welding quality, which is more difficult for laser - arc hybrid welding to achieve.

In the extant literature landscape of AZ31B magnesium alloy welding research, the majority of published works have bifurcated their focus. On one hand, investigations have predominantly centered around the butt-welding of thick AZ31B magnesium alloys, where the material thickness is ≥1.5mm, delving into the complex metallurgical processes and mechanical property outcomes associated with such configurations. On the other hand, considerable attention has been given to the lap-welding of thin AZ31B magnesium alloys, with a thickness of ≤1.5mm, exploring the challenges and optimal parameters specific to this joining technique. However, a conspicuous research gap persists regarding the butt-welding of 1mm thick AZ31B sheets, which is of particular significance as thin magnesium alloys are increasingly sought after in high-tech and lightweight applications.

This work endeavors to bridge this knowledge chasm by meticulously comparing the butt-welding scenarios of 1mm thick AZ31B sheets with and without the application of an oscillating beam. The employment of an oscillating beam during laser welding is hypothesized to exert a profound influence on the weld pool dynamics, potentially enhancing the homogeneity of heat distribution through modulating fluid flow patterns within the molten pool. By virtue of this, we anticipate improved fusion characteristics, reduced defect formation probabilities such as porosity and cracking, and ultimately, enhanced mechanical properties of the welded joints.

2. Experimental Procedure

2.1. Experimental material

Material used in this study was 1 mm-thick AZ31B magnesium alloy sheets with dimensions of 120×50 mm. The chemical composition and tensile properties are detailed in Table 1.

Prior to welding, the sheets were mechanically brushed using and chemically cleaned with, removing oxidation layers and oil residues on the metal surface. Subsequently,the sheets were assembled in a butt-joint configuration.

2.2. Welding parameters

The experimental setup incorporated a YLS-10000-S4 fiber laser equipped with a D50 laser head and integrated with a KR60HA robotic arm. The maximum laser power output was 10 kW, with a wavelength of 1064 nm, and the laser beam was focused to a spot diameter of precisely 0.4 mm. Additionally, argon gas shielding was applied to both the top and root surfaces of the weld at flow rates of 25 L/min and 20 L/min, respectively. The schematic diagram of the welding process is depicted in Figure 1.

In this investigation, circular beam oscillation was employed to optimize the welding process. The welding parameters are provided in Table 2. After welding, metallographic samples, scanning electron microscope (SEM) specimens, and tensile test specimens were prepared, as illustrated in Figure 2. The metallographic samples were initially ground using silicon carbide abrasive papers, followed by chemical polishing with a solution comprising 95ml deionized water, 5ml hydrofluoric

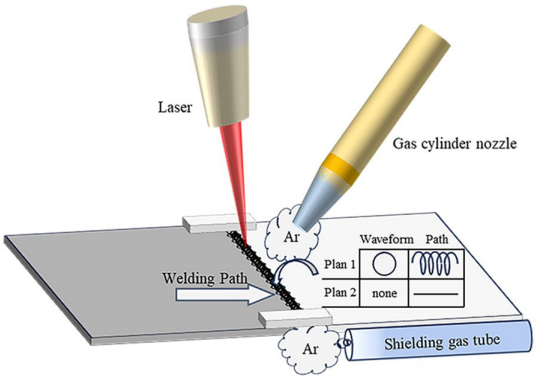

Figure 1. The schematic diagram of laser welding.

Table 1. Chemical composition of AZ31B magnesium alloy.

Chemical composition(wt.%)							Mechanical properties	
Al	Si	Ca	Zn	Mn	Cu	Mg	UTS/MPa	EL/%
2.9	0.07	0.04	1.1	0.3	0.01	Bal.	287	8.5

acid, and 1g oxalic acid. The microstructural characterization was performed using optical microscope (OM) and VHX-6000 Ultra-Depth Three-Dimensional Microscope (UDTM). Tensile tests were conducted using Mini-MTS@HT in-situ biaxial tensile testing machine. Specimens for tensile testing were extracted from the base metal and weld seams using electric discharge machining (EDM) wire cutting. The tensile testing was performed at a constant speed of 0.6 mm/min, and multiple specimens were tested in each group to ensure statistical reliability.

2.3. Test details

Hardness measurements were carried out using a Vickers microhardness tester, with indentations made at fixed intervals from the base metal to the weld seam. Fracture surface observations were conducted using Tescan Vega3 scanning electron microscope at magnifications of 200× and 400×. The hardness of the base metal and weld zone was evaluated using an HM2000 microhardness tester, with an applied load of 100 gf for indentation during hardness testing.

3.Results and Discussion

3.1. Macro morphology of the welded joint

Figure 2 illustrates the comparison between the direct laser weld joint (a) and the oscillating laser weld joint (b). As shown in Figure 2a, the weld exhibits a notably irregular shape with serrated undulations along its edges. This irregularity suggests that during direct laser welding, the laser energy is concentrated, leading to uneven localized melting and solidification in the weld pool. In contrast, the weld seam in Figure 2b appears more uniform and smoother. The oscillation of the laser beam facilitates a more even distribution of laser energy across the welding zone, resulting in a more consistent and regular weld seam formation.

Figure 2c and Figure 2d respectively present the three-dimensional views of non-oscillatory laser welds and oscillatory laser welds. From the figures, it is evident that the oscillatory laser weld exhibits a greater width compared to the non-oscillatory weld. In the case of the non-oscillatory laser weld, the penetration depth at the center is greater than that at the edges, with a relatively smooth depth variation. In contrast, the oscillatory laser weld shows depth fluctuations, with multiple regions exhibiting greater penetration. These differences are attributed to the heat dispersion and stirring effect of the molten pool caused by laser oscillation. The impacts of these distinctions are not limited to macroscopic morphology; they also influence the microstructure.

As a result of the highly concentrated heat input during direct laser welding, a steep temperature gradient forms within the weld and its heat-affected zone (HAZ), which may promote the formation of relatively coarse grains during the cooling process.

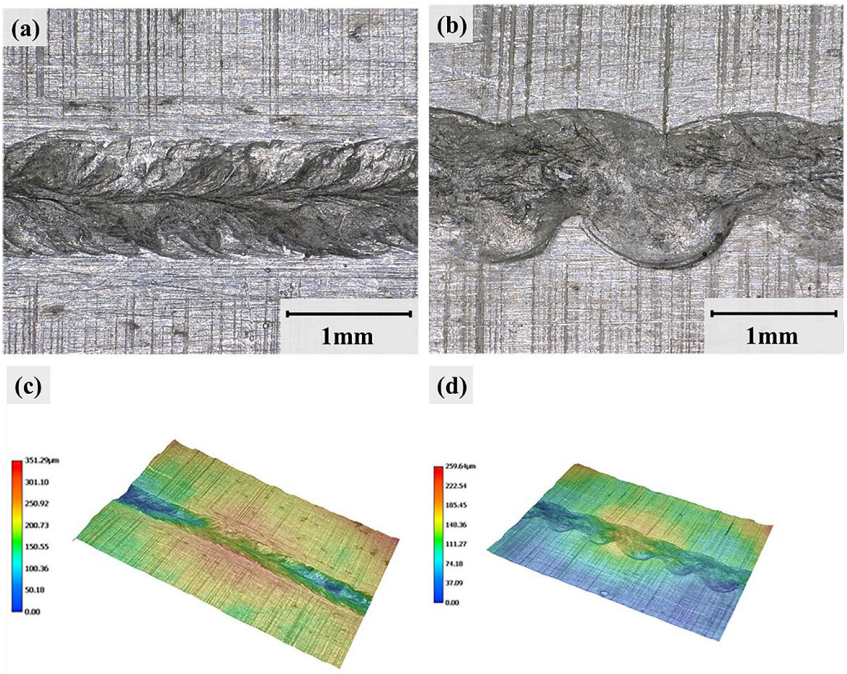

Figure 2. Macroscopic Morphologies and Cross Sections of Two Different Welds, (a) Non-oscillating Welding, (b) Oscillating Welding, (c) 3D view of Non-Oscillating joint, (d) 3D view of oscillating Welding.

Table 2. Parameters of laser welding process in experiments.

Joint number	Laser power/W	Welding speed/ (m/min)	Focal position/ mm	Oscillation pattern	Oscillation radius/mm	Oscillation frequency/Hz
1	800	4	0	none	0	0
2	800	4	0	circle	0.5	50

3.2. Microstructure of the welded joint

The super depth-of-field optical micrographs of the laser welding of AZ31B magnesium alloy are shown in Figure 3. In Figure 3a, the heat-affected zone and fusion zone (FZ) of the non-oscillating laser weld are depicted. Near the fusion line, there are columnar crystals that predominantly align in the same direction, while in the central area of the weld, equiaxed crystals appear. The temperature gradient at the molten pool boundary is substantial, and the cooling rate is rapid, causing the columnar crystals to grow along the direction of heat flow. This results in the alignment of the columnar crystals. Figure 3b presents the metallographic photograph of the middle part of the non-oscillating laser weld. A significant presence of equiaxed grains can be observed in the figures. This is because the weld center is far from the base metal, resulting in a lower temperature gradient. Consequently, the directional growth of crystals is reduced, leading to the formation of an equiaxed grain zone at the weld center. Figure 3c shows the metallographic photograph near the fusion line of the oscillating laser weld. Compared to the non-oscillating laser weld, near the fusion line, the orientation of columnar grains appears relatively disordered. The closer to the weld center, the more disorganized the columnar grains become, and regions with a mixture of equiaxed and columnar grains start to appear. Compared to non-oscillatory laser welds, equiaxed grains are observed earlier in oscillatory laser welds. In Figure 3d, the metallographic photograph of the middle part of the oscillating laser weld reveals a diverse grain structure. At the weld center, equiaxed grains, fine columnar grains, and dendritic equiaxed structures resembling snowflake patterns are observed.The oscillation of the laser introduces a dynamic heat input mode that modifies the local temperature gradient. Additionally, as the laser undergoes periodic circular oscillations, it stirs the molten pool, leading to complex convection effects within the pool. These convection flows mix the grains, resulting in the appearance of various grain types in the weld center.In addition ,these convection flows lead to the disorientation of columnar grains near the fusion line and the formation of mixed regions containing both equiaxed grains and columnar grains.

In oscillatory laser welds, in addition to fine columnar grains and equiaxed grains, numerous snowflake-like equiaxed dendrites can be observed at the weld center. The growth process of these equiaxed dendrites is illustrated in Figure 4. Near the fusion line, the equiaxed dendrites grow toward the weld center to a limited extent. However, due to molten pool stirring and vortex effects caused by laser oscillation, the dendrites are broken into smaller fragments[16]. The fragmented parts are then rapidly transported to the weld center, where they act as new nucleation sites. Additionally, repetitive laser-induced heating of the molten pool extends the holding time, which reduces the temperature gradient at the weld center. The new nucleation sites grow without pronounced directionality, ultimately forming snowflake-like equiaxed dendrites.

Figure 5 and Figure 6 show the results of area scanning and point scanning at the weld region of the base metal, respectively. Identical strengthening phases were identified in the base metal and both types of welds. In the scanning electron microscope (SEM) observations of the base metal, the strengthening phases were found to be more abundant and continuously distributed. However, in the welds, the quantity of strengthening phases was lower, and their size was smaller. The analysis indicates that α-Mg and $Mg_{17}Al_{12}$ are the primary components of both the welds and the base

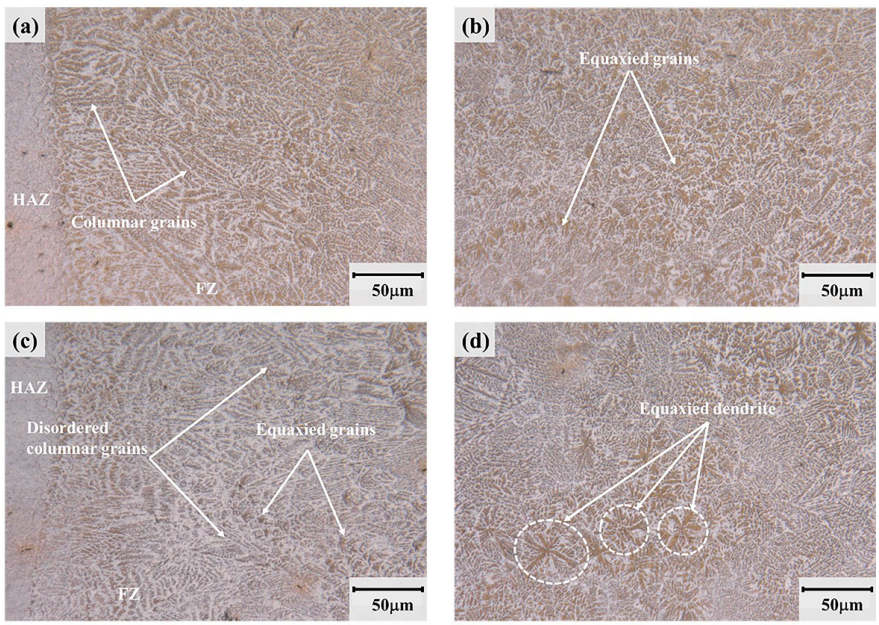

Figure 3. Microstructure of the weld observed under a depth-of-field microscope:(a)microstructure neighboring the fusion line of the weld without oscillation,(b)Middle of weld without oscillation,(c)microstructure neighboring the fusion line of the weld with circle oscillation,(d)Middle of weld with circle oscillation.

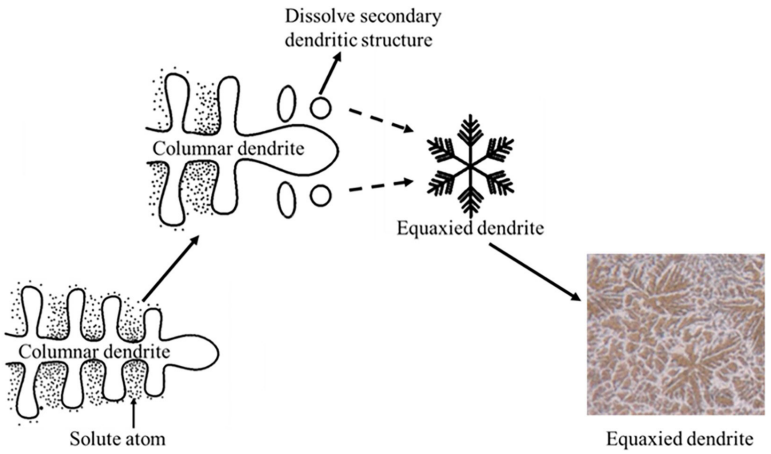

Figure 4. Schematic diagram of the growth mechanism of equiaxed dendrites[16].

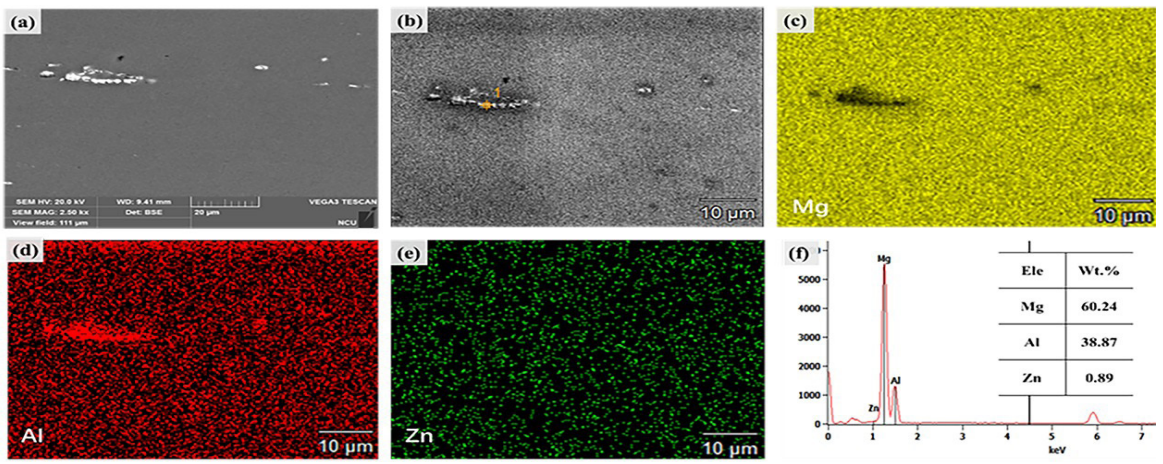

Figure 5. Analysis results of area scanning and point scanning for the base metal.

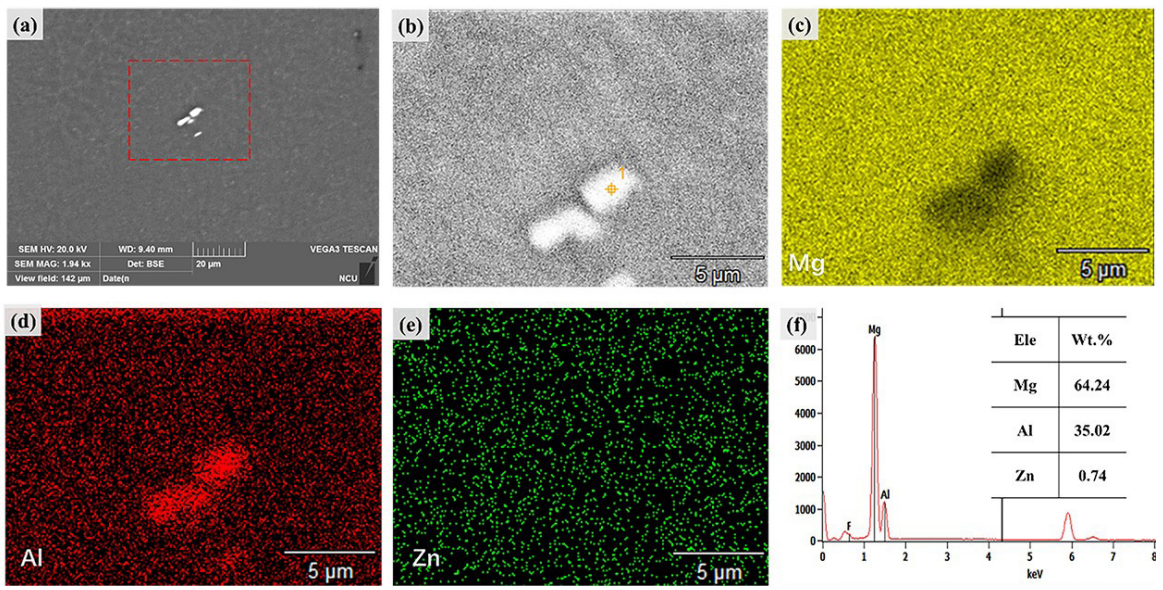

Figure 6. Analysis results of area scanning and point scanning for the welds.

metal, with only slight compositional differences between the two types of welds.

3.3. Mechanical perfoormance of the joint

The tensile specimens, obtained by wire cutting from the welded parts of AZ31B magnesium alloy after laser welding treatment, are shown in Figure 7, with the corresponding tensile results presented in Figure 8. All specimens from both welding processes fractured at the weld seams during the tensile testing. Analysis of the tensile data reveals that both welding methods demonstrate high tensile strengths. The base metal exhibits the highest tensile strength, followed by the welded joints using the laser oscillating welding process, while the non-oscillating laser welding joints demonstrate the lowest strength. Specifically, the tensile strength of the laser oscillating welding reaches approximately 85% of the base metal's strength, whereas the non-oscillating welding achieves about 76%. Compared to the non-oscillating welding, the laser oscillating welding produces a higher strain; however, the strain levels for both methods are still lower than that of the base metal. Notably, the strain ratio for the laser oscillating welding, when compared to the base metal, is significantly higher than that for the non-oscillating welding.

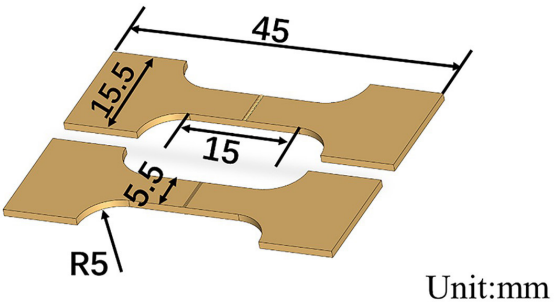

Figure 7. Specifications of Tensile Specimens.

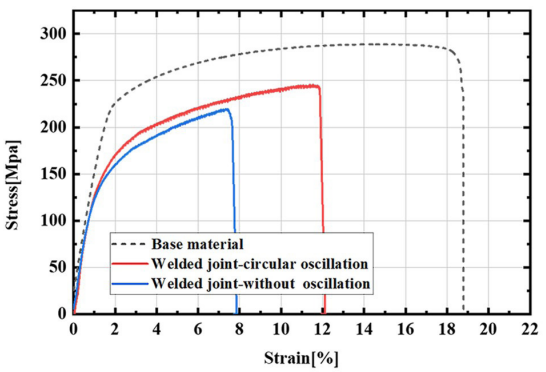

Figure 8. Stress-Strain Curves of Tensile Tests for the Base Metal and Welds with and without Oscillation.

3.4. Fracture morphology of the joint

Figure 9 shows the fracture SEM images of three types of AZ31B materials. Figure 8a displays the fracture surface and a partially magnified view of the base metal. Figure 8b presents the fracture surface and a partial magnification of the non-oscillating laser-welded joints, while Figure 8c shows the fracture surface and a partial magnified view of the oscillating laser-welded joints. It is evident from the figure that fracture surfaces feature dimples of all three materials, indicating that plastic deformation occurred during the fracture process. However, defects such as pores are visible in both types of welds (b) and (c). Notably, the non-oscillating laser-welded joints (b) exhibit a higher number of pores compared to the oscillating laser-welded joints (c). Since pores can act as stress concentration points, they promote fracture at lower stress levels. As a result, the tensile strength and toughness of the non-oscillating laser-welded joints (b), which have a greater number of pores, are lower than those of the oscillating laser-welded joints (c). This difference can be attributed to the more uniform heat input during the laser oscillation process, where the oscillation of the laser beam helps stir the molten pool, improving its fluidity, facilitating gas release, and reducing the formation of bubbles.

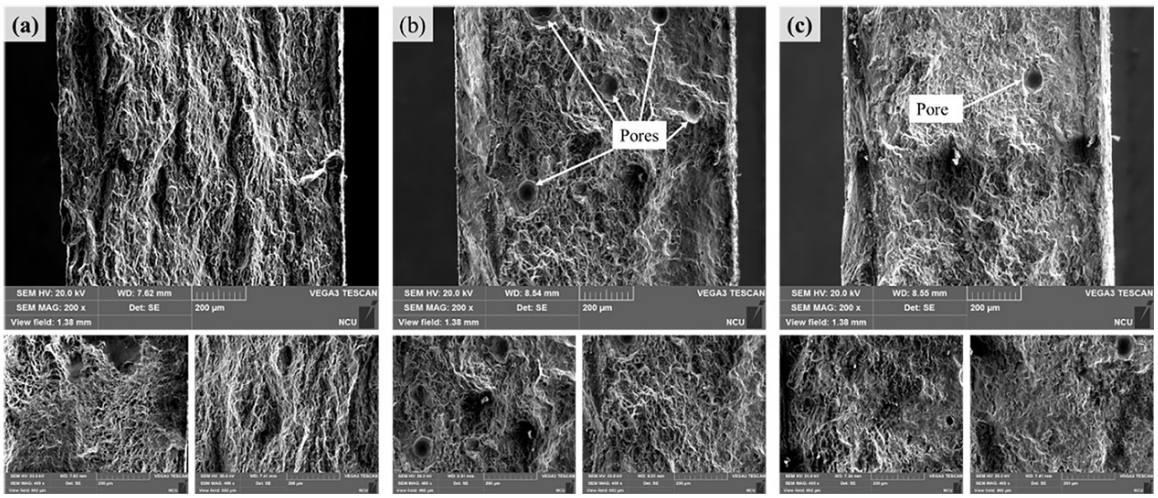

Figure 9. Fracture Surface Morphology:(a) Base Metal,(b) Non-oscillating Welding,(c) Oscillating Welding.

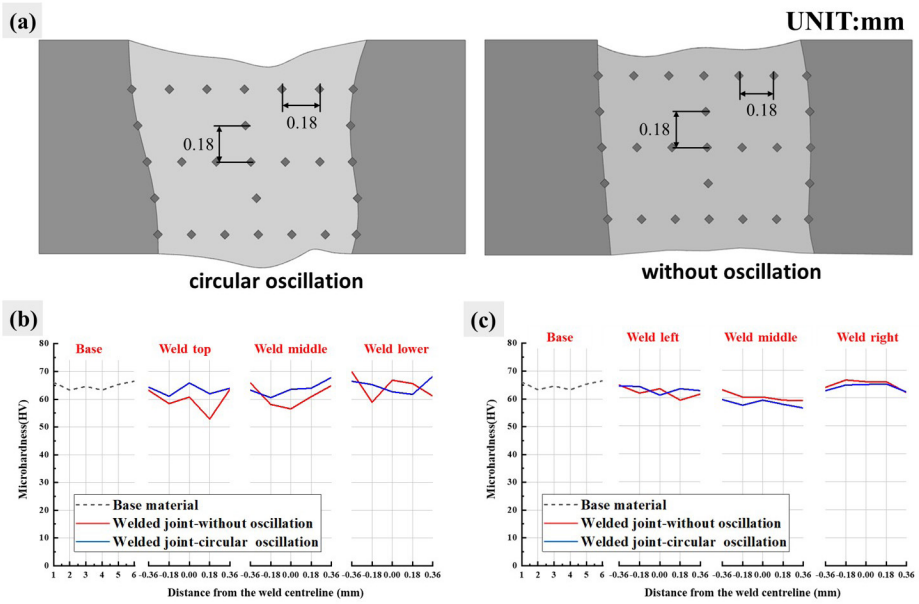

Figure 10. The microhardness of the base metal and different weld seam positions with and without oscillation. (a) Distribution diagram of hardness measurement points; (b) Comparison of transverse hardness in the weld; (c) Comparison of longitudinal hardness in the weld.

3.5. Microhardness of the joint

Figure 10 shows the hardness profiles of AZ31B magnesium alloy laser welds. It can be observed that the hardness of the welds produced by both welding methods is similar to that of the base metal. Notably, the hardness at the top and middle sections of the welds is slightly higher in circular oscillation welding compared to non-oscillatory welding, while the hardness at the bottom of the welds is nearly identical for both methods. This difference arises because non-oscillatory laser welding concentrates heat, leading to faster grain growth in the weld zone. In materials science, rapid grain growth typically results in reduced hardness. In circular oscillation laser welding, the distributed heat input results in relatively slower grain growth and the formation of finer grains. The refined grain structure inhibits dislocation movement, thereby enhancing the material's hardness. As a result, the hardness in the top and middle sections of oscillation welds is higher than that of non-oscillatory welds.

Figure 10b is a comparison of transverse hardness, and Figure 10c is a comparison of longitudinal hardness. It can be observed that the hardness of the welds produced by both welding methods is similar to that of the base metal. In terms of transverse hardness,the hardness at the top and middle sections of the welds is slightly higher in circular oscillation welding compared to non-oscillatory welding, while the hardness at the bottom of the welds is nearly identical for both methods. In terms of longitudinal hardness, both welding methods show similar hardness near the fusion line. However, near the weld centerline, the hardness of the non-oscillatory weld is higher than that of the oscillatory laser weld.

The difference arises because, in materials science, rapid crystal growth generally reduces hardness. In the transverse hardness comparison, the oscillatory laser welding results in slower crystal growth due to repeated heating of the molten pool, leading to higher hardness in the upper and middle regions. The lower part of the weld is less affected, so the hardness difference between the two welding methods is not significant. In the longitudinal direction, near the centerline of the non-oscillatory weld, there are more equiaxed grains. In contrast, in the oscillatory laser weld, the stirring of the molten pool leads to a greater variety of crystal types in the weld center, affecting the hardness in that region. Therefore, the hardness near the centerline is higher in the non-oscillatory weld.

4. Conclusion

- (1) The application of laser beam oscillation technology during butt welding of 1 mm thick AZ31B Mg alloy sheets effectively enhanced weld seam uniformity, refined the microstructure, and significantly reduced welding defects such as porosity. Consequently, the tensile strength of the oscillation-welded joint reached 85% of the base metal (BM), demonstrating a clear advantage over non-oscillation welding (76% of BM).
- (2)Regardless of beam oscillation, the laser welding process resulted in a significant reduction in the tensile elongation of AZ31B Mg alloy welded joints compared to the BM. This indicates that the thermal cycle inherent to laser welding causes irreversible damage to the material's plasticity, establishing it as a critical constraint on the toughness of welded structures.
- (3) Fractographic analysis revealed fewer pores in oscillation-welded specimens, with distinct micro-morphological features compared to non-oscillation welds. This directly verifies, at the

fracture mechanism level, the effectiveness of beam oscillation in suppressing welding defects and enhancing joint integrity.

5. Acknowledgments

This work is supported by the Joint Research Fund in Astronomy (U1731118) uder cooperative agreement between the National Natural Science Foundation of China (NSFC) and Chinese Academy of Sciences (CAS)”

6. References

1. Cao X, Jahazi M, Immarigeon JP, Wallace W. A review of laser welding techniques for magnesium alloys. J Mater Process Technol. 2006;171(2):188-204. http://doi.org/10.1016/j.jmatprotec.2005.06.068.
2. Xu T, Yang Y, Peng X, Song J, Pan F. Overview of advancement and development trend on magnesium alloy. J Magnes Alloy. 2019;7(3):536-44. http://doi.org/10.1016/j.jma.2019.08.001.
3. Zhou W, Aprilia A, Mark CK. Mechanisms of cracking in laser welding of magnesium alloy AZ91D. Metals. 2021;11(7):1127. http://doi.org/10.3390/met11071127.
4. Jiang P, Dong H, Cai Y, Gao M. Effects of laser power modulation on keyhole behavior and energy absorptivity for laser welding of magnesium alloy AZ31. Int J Adv Manuf Technol. 2023;125(1-2):563-76. http://doi.org/10.1007/s00170-022-10586-5.
5. Zou J, Gong J, Han X, Zhao Y, Wu Q. In situ detection of plume particles in intelligent laser welding. Mater Des. 2022;217:110633. http://doi.org/10.1016/j.matdes.2022.110633.
6. Xu Y, Qian P, Qiao Y, Li J, Zhang J. Study on laser welding process, microstructure and properties of AZ31B magnesium alloy. Trans Indian Inst Met. 2022;75(11):2905-12. http://doi.org/10.1007/s12666-022-02659-6.
7. Zhang M, Wu J, Mao C, Cheng B, Shakhawat HMD, Li H, et al. Impact of power modulation on weld appearance and mechanical properties during laser welding of AZ31B magnesium alloy. Opt Laser Technol. 2022;156:108490. http://doi.org/10.1016/j.optlastec.2022.108490.
8. Hao K, Wang H, Gao M, Wu R, Zeng X. Laser welding of AZ31B magnesium alloy with beam oscillation. J Mater Res Technol. 2019;8(3):3044-53. http://doi.org/10.1016/j.jmrt.2019.04.024.
9. Zhang M, Duan W, Zhang J, Wang R, Li H, Cheng B, et al. Formation and mechanical properties of AZ31B magnesium alloy welds by power-modulated oscillating laser. Opt Laser Technol. 2024;179:111421. http://doi.org/10.1016/j.optlastec.2024.111421.
10. Jiang Y, Jiang M, Chen X, Chen A, Ma S, Jiang N, et al. Vacuum laser beam welding of AZ31 magnesium alloy: weld formability, microstructure and mechanical properties. Opt Laser Technol. 2024;169:110115. http://doi.org/10.1016/j.optlastec.2023.110115.
11. Lei Z, Bi J, Li P, Guo T, Zhao Y, Zhang D. Analysis on welding characteristics of ultrasonic assisted laser welding of AZ31B magnesium alloy. Opt Laser Technol. 2018;105:15-22. http://doi.org/10.1016/j.optlastec.2018.02.050.
12. Chen M, Xu J, Xin L, Zhao Z, Wu F, Ma S, et al. Effect of keyhole characteristics on porosity formation during pulsed laser-GTA hybrid welding of AZ31B magnesium alloy. Opt Lasers Eng. 2017;93:139-45. http://doi.org/10.1016/j.optlaseng.2017.01.018.
13. Gao Y, Hao K, Xu L, Han Y, Zhao L, Ren W, et al. Microstructure homogeneity and mechanical properties of laser-arc hybrid welded AZ31B magnesium alloy. J Magnes Alloy. 2024;12(5):1986-95. http://doi.org/10.1016/j.jma.2022.09.034.
14. Hao K, Gao Y, Xu L, Han Y, Zhao L, Ren W, et al. Beam oscillating parameters on pore inhibition, recrystallization and grain boundary characteristics of laser-arc hybrid welded AZ31 magnesium alloy. J Magnes Alloy. 2024;12(6):2489-502. http://doi.org/10.1016/j.jma.2022.10.010.
15. Meng Y, Fu J, Zhang S, Gong M, Gao M, Chen H. Laser-arc hybrid welding of AZ31B magnesium alloy by newly-designed beam oscillating pattern. J Manuf Process. 2023;93:208-18. http://doi.org/10.1016/j.jmapro.2023.03.028.
16. Gao M, Wang H, Hao K, Mu H, Zeng X. Evolutions in microstructure and mechanical properties of laser lap welded AZ31 magnesium alloy via beam oscillation. J Manuf Process. 2019;45:92-9. http://doi.org/10.1016/j.jmapro.2019.07.001.

Data Availability

The entire dataset supporting the results of this study was published in the article itself.